Bioorganic & Medicinal Chemistry 18 (2010) 6080–6088

Contents lists available at ScienceDirect

Bioorganic & Medicinal Chemistry

journal homepage: www.elsevier.com/locate/bmc

Dimethylaminopyridine derivatives of lupane triterpenoids are potent disruptors of mitochondrial structure and function

Jon Holy [a,*], Oksana Kolomitsyna [b], Dmytro Krasutsky [b], Paulo J. Oliveira [c], Edward Perkins [d], Pavel A. Krasutsky [b]

[a] Department of Anatomy, Microbiology and Pathology, University of Minnesota School of Medicine, Duluth, USA
[b] Natural Resources Research Institute, University of Minnesota, Duluth, USA
[c] Center for Neurosciences and Cell Biology, University of Coimbra, Coimbra, Portugal
[d] Mercer School of Medicine, Savannah, GA, USA

ARTICLE INFO

Article history:
Received 8 May 2010
Revised 16 June 2010
Accepted 18 June 2010
Available online 1 July 2010

Keywords:
Lupane triterpenoid
Dimethylaminopyridine
Mitochondria
Cell proliferation
Melanoma

ABSTRACT

Development of mitochondrially-targeted drugs is receiving increasing attention because of the central roles these organelles play in energy production, reactive oxygen generation, and regulation of cell death pathways. Previous studies have demonstrated that both natural and synthetic triterpenoids can disrupt mitochondrial structure and function. In this study, we tested the ability of a number of dimethylaminopyridine (DMAP) derivatives of lupane triterpenoids to target mitochochondria in two human melanoma cell lines and an untransformed normal fibroblast line. These compounds induced a striking fragmentation and depolarization of the mitochondrial network, along with an inhibition of cell proliferation. A range of potencies among these compounds was noted, which was correlated with the number, position, and orientation of the DMAP groups. Overall, the extent of proliferation inhibition mirrored the effectiveness of mitochondrial disruption. Thus, DMAP derivatives of lupane triterpenoids can be potent mitochondrial perturbants that appear to suppress cell growth primarily via their mitochondrial effects.

1. Introduction

Natural products have played major roles in the development of medically useful drugs. Triterpenoids are a very large and interesting family of compounds, many members of which exhibit biological activity in mammalian cells, including cytotoxic, antitumor, antiviral, antifungal, and anti-inflammatory effects.[1,2] Potential uses include developing triterpenoids as anti-cancer drugs, both as chemopreventatives and as chemotherapeutics. Early interest in this area was generated by the discovery that the lupane triterpenoid betulinic acid (BA) displays a notable level of discrimination in promoting apoptosis of melanoma cells.[3] Subsequent studies showed that BA also exhibits activity against glioma, ovarian carcinoma, small-cell and non-small cell lung carcinomas, and cervical carcinoma cell lines.[4–6] Interestingly, cells of neuroectodermal origin appear to be especially sensitive to this pentacyclic triterpenoid.[7–9] Oleanane, ursane, and a number of other types of triterpenoids are also being investigated as anti-cancer agents,[10] and increasing attention is being given toward the production of synthetic triterpenoid derivatives. In particular, substantial efforts have been invested in developing 2-cyano-3,12-dioxooleana-1,9(11)-dien-28-oic (CDDO) derivatives of oleanolic acid as therapeutic agents. The activity of CDDO and imidazolide, amide, and dinitrile derivatives on the behavior of a variety of solid tumors and leukemias has been documented, and a methyl ester of CDDO is in clinical trials.[11]

The activities of a number of signaling networks have been shown to be altered by triterpenoids, including NfκB, NRF2, TGFβ, ERK, STAT, Akt, mTOR, PPARγ, and AMPK pathways.[11–16] Induction of apoptosis or autophagy is frequently reported in studies of triterpenoid action, but chemoprotective effects have also been reported. Notably, the net effects of a number of triterpenoids appear to be centered around disruption of mitochondrial function. Events associated with these compounds include generation of reactive oxygen species (ROS), both pro- and anti-oxidant functions and disruption of redox status, calcium deregulation, a decrease in mitochondrial membrane potential, and cytochrome C release.[6,11] From a chemotherapeutic perspective, actions that target mitochondria are of particular interest as they could be of use in promoting apoptosis in malignant cells.

Mitochondria are recognized to play pivotal roles in transducing or amplifying signals to cell death pathways, and are thus attractive cancer chemotherapeutic targets. Multiple subgroups of triterpenoids (including lupane, oleane and ursane triterpenoids) have been reported to perturb mitochondria, but relatively little information is available on actual mechanisms of action, or how specific functional groups affect mitochondrial dynamics. As part

* Corresponding author. Tel.: +1 218 726 8885.
E-mail address: jholy@d.umn.edu (J. Holy).

0968-0896/$ - see front matter © 2010 Elsevier Ltd. All rights reserved.
doi:10.1016/j.bmc.2010.06.075

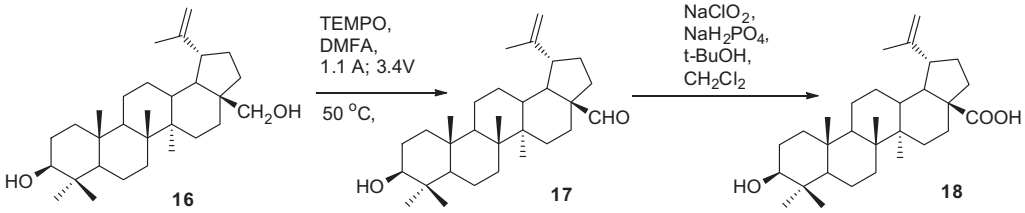

Scheme 1. Synthesis of betulinic acid (**18**).

of our efforts in examining a number of natural and semi-synthetic derivatives of lupane triterpenoids for bioactivity, we found that quaternary salt (QUAT) dimethylaminopyridine (DMAP) derivatives of pentacyclic triterpenes dramatically alter mitochondrial structure and function and suppress cell proliferation. Structure–activity studies indicate that the mitochondrial effects of these compounds are not simply a consequence of the presence of DMAP groups, but are dependent on the specific numbers and orientations of these groups. These findings reveal that DMAP derivatives of lupane triterpenoids constitute a novel category of mitochondrial poisons that may have utility as research and biomedical tools.

2. Results and discussion

2.1. Chemistry

Birch bark lupane triterpenoids betulin (**16**) and betulinic acid (**18**) have been chosen as basic natural precursors for synthesis of dimethylaminopyridinium QUATS.[1] Betulin with 99% + purity was isolated from the extract of outer birch bark of *Betula papyrifera*—the North American commercial birch tree—in accordance with a previously developed procedure.[17] Betulinic acid (**18**) was synthesized by a recently developed two step process (Scheme 1).[18] The first step is the selective *N*-oxyl-mediated electrooxidation of betulin (**16**) into betulinic aldehyde (**17**) with TEMPO in dimethylformamide. The betulin aldehyde was subsequently converted to betulinic acid with $NaClO_2$ or $KClO_2$. These methods are proposed as the most convenient for betulinic acid synthesis in the laboratory as well as for industrial scales. Pilot tests of these methods have been successfully conducted in our laboratory in a 50-L apparatus which was equipped with graphite (anode) and copper (cathode) electrodes.

Betulin (**16**) and betulinic acid (**18**) were converted to DMAP derivatives (**1–15**) through intermediate acylation of corresponding hydroxy groups at C3- and C28-carbons with the chloroacids and bromoacids shown in Scheme 2. As a result, corresponding C3 and C28 chloro and bromoacylates were produced as precursors for DMAP derivatives. Bromination with 2,2′-azobisisobutyronitrile in CCl_4 was performed for subsequent synthesis of C28 quaternary salts of DMAP. It is necessary to note that betulinic acid (**2**) may not be selectively brominated with AIBN, because very low solubility in CCl_4. Therefore this process was provided through intermediate acylation of betulinic acid (**2**) with trifluoroacetic acid. Then, 3-trifluoroacetate of betulinic acid was selectively brominated at C29-carbon. Subsequent soft hydrolysis of this trifluoroacetate with 5% NaOH in THF at rt yielded to 30-bromobetulinic acid as a precursor for corresponding DMAP derivative of betulinic acid (**18**). All tested DMAP derivatives have been characterized with ^1H and ^{13}C NMR spectra and HRMS-analyses.

Fifteen lupane triterpenoid–dimethylaminopyridinium (LT–DMAP) derivatives (Fig. 1) of betulin and betulinic acid were produced by the Scheme 2. The LT–DMAP compounds **1–15** were prepared as stock solutions in dimethylsulfoxide (DMSO), and added to culture medium, such that the final concentration of DMSO never exceeded 0.2%. Control groups received vehicle (DMSO) only, corresponding to the highest concentration used (0.2%). Synthesized compounds and their precursors revealed a remarkable level of anti-bacterial[19] and anti-proliferative activity[20] in previous studies.

2.2. Cell lines and cell culture

WM3211 radial-phase and WM793 vertical-phase human melanoma cells were the kind gifts of Dr. Meinhard Herlyn (WISTAR Inst.). BJ fibroblasts were obtained from ATCC. Cells were cultured in high-glucose Dulbecco's modified Eagles medium (DMEM) containing 8% Fetal Clone III (HyClone, Logan, UT), 3.5% horse serum (Gibco) and 5 mM Glutamax (Invitrogen). Cells were passaged and prepared for experiments using standard trypsin-EDTA methods.

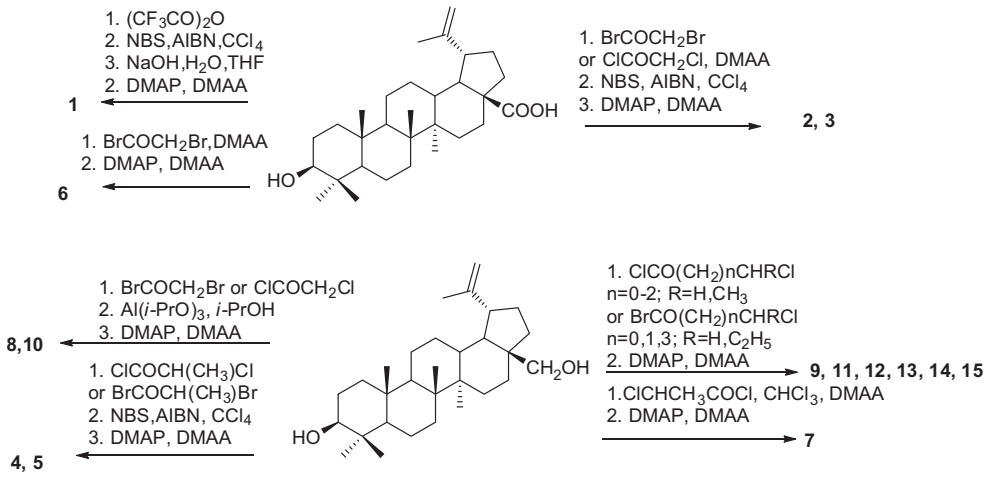

Scheme 2. Synthesis of LT–DMAPs (**1–15**).

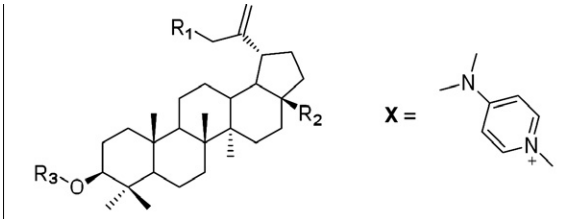

R_1= X^+Br^-; R_2= COOH; R_3=H **(1)**
R_1= X^+Br^-; R_2= COOH; R_3= $OCOCH_2X^+Br^-$ **(2)**
R_1= X^+Br^-; R_2= COOH; R_3= $OCOCH_2X^+Cl^-$ **(3)**
R_1= X^+Br^-; R_2= $CH_2OCOCH(CH_3)X^+Cl^-$; R_3= $OCOCH(CH_3)X^+Cl^-$ **(4)**
R_1= X^+Br^-; R_2= $CH_2OCOCH(CH_3)X^+Br^-$; R_3= $OCOCH(CH_3)X^+Br^-$ **(5)**
R_1=H; R_2= COOH; R_3= $OCOCH_2X^+Br^-$ **(6)**
R_1=R_3=H; R_2= $CH_2OCOCH(CH_3)X^+Cl^-$ **(7)**
R_1=H; R_2= CH_2OH; R_3= $OCOCH_2X^+Br^-$ **(8)**
R_1=H; R_2= $CH_2OCO(CH_2)_3X^+Br^-$; R_3= $OCO(CH_2)_3X^+Br^-$ **(9)**
R_1=H; R_2= CH_2OH; R_3= $OCOCH_2X^+Cl^-$ **(10)**
R_1=H; R_2= $CH_2OCO(CH_2)_2X^+Cl^-$; R_3= $OCO(CH_2)_2X^+Cl^-$ **(11)**
R_1=H; R_2= $CH_2OCOCH(C_2H_5)X^+Br^-$; R_3= $OCOCH(C_2H_5)X^+Br^-$ **(12)**
R_1=H; R_2= $CH_2OCOCH(CH_3)X^+Cl^-$; R_3= $OCOCH(CH_3)X^+Cl^-$ **(13)**
R_1=H; R_2= $CH_2OCOCH_2X^+Br^-$; R_3=$OCOCH_2X^+Br^-$ **(14)**
R_1=H; R_2= $CH_2OCOCH_2X^+Cl^-$; R_3= $OCOCH_2X^+Cl^-$ **(15)**

Figure 1. The 15 LT–DMAP compounds synthesized by Schemes 1 and 2.

2.3. Proliferation assays

Sulforhodamine B assays were carried out essentially as described by Skehan et al.[21] Cells were seeded in 48-well plates (20,000 cells/ml) and allowed to recover for 24 h prior to addition of LT–DMAPs. Serial 1:1 dilutions of compounds from 2 mg/ml stock solutions in DMSO, spanning from 0.25 to 4 μg/ml were added, and plates subsequently incubated for 72 h. Vehicle-only control wells received 0.2% DMSO, which corresponded to the amount delivered with the highest concentration of compound tested (4 μg/ml). Plates were gently rinsed twice with PBS, and then cells were fixed overnight with freezer-temperature (−10 °C) absolute methanol and 1% acetic acid. Fixative was decanted and the plates allowed to air dry prior to the addition of 0.5% SRB in 1% acetic acid. Cells were stained for 30 min at rt, and then gently rinsed three times with 1% acetic acid and air dried. SRB was eluted from the cells with 10 mM Tris, pH 10, and the absorbance at 540 nm measured with a Synergy (Bio-Tek) multiplate reader.

2.4. Effects of LT–DMAPs on mitochondrial structure and function

Tetramethylrhodamine methylester (TMRM) and related probes have been used extensively for detecting changes in mitochondrial membrane polarization, as well as displaying the morphology of polarized mitochondria. In this study, TMRM labeling of intact cells demonstrates that a number of differences exist in the mitochondrial networks of the WM3211 radial-phase and WM793 vertical-phase melanoma cell lines. WM3211 cells generally display dense masses of short mitochondria, whereas vertical-phase WM793 cells exhibit a more diffuse network of elongated mitochondria (Figs. 2 and 3). In addition, the overall intensity of mitochondrial labeling is somewhat less intense in WM793 cells. Initial screening of a number of lupane triterpenoid–dimethylaminopyridine conjugates (LT–DMAPs) in these cell lines revealed that mitochondrial structure and polarization were radically altered by some of these compounds. At up to 4 μg/ml, the highest concentration tested, the effects of LT–DMAPs range from no discernable effects, to complete vesiculation and depolarization of mitochondria, depending on the compound (Fig. 2). Compounds **1–5** are very weak mitochondrial perturbants, and have little noticeable effect on either mitochondrial polarization or morphology. Compounds **6–10** are intermediate in strength, and can be roughly ordered based on strength of mitochondrial effects (**6** < **10** < **8** < **9** < **7**). In general, the radial-phase WM3211 melanoma cells are more sensitive to these compounds than the WM793 vertical-phase cells. Mitochondria of both cell lines exposed to 4 μg/ml of **6** remain strongly polarized, but WM3211 mitochondria begin to round up and appear more spherical. Interestingly, some WM793 cells treated with this concentration of **6** appear brighter than controls, suggesting some hyperpolarization of mitochondrial membranes may be occurring in this cell line. Compound **10** reduces mitochondrial polarization in both cell lines, with a relatively stronger effect on WM3211s. In addition, cytoplasmic vacuolization occurs in WM793 cells, and co-localization studies demonstrate that many of these vacuoles are derived from mitochondria, based on TMRM fluorescence (Fig. 3). Little vacuolization is apparent in WM3211 cells treated with 4 μg/ml of **10**. In both cell lines, compounds **8** and **9** clearly depolarize mitochondria, with the greatest effects again appearing in WM3211 cells. Mitochondria are extensively fragmented, and depolarization is almost complete at this concentration and timepoint of compound **7**. In addition, extensive cytoplasmic vacuolization occurs in both cell lines, with the most prominent effects displayed by WM793 cells. Compounds **11–15** result in essentially complete mitochondrial fragmentation and depolarization in both cell lines at concentrations under 4 μg/ml within a few hours of treatment. Some cytoplasmic vacuolization is occasionally present, but occurs to a much more limited extent than with **7** and **10**.

The fragmentation and vesiculation of mitochondria induced by LT–DMAPs resembles the 'thread-grain' transition described by Skulachev et al.[22] Fragmentation of the mitochondrial network has been shown to result from treatment with respiratory inhibitors, uncouplers, and oxidative stress, and involves the dynamin-related GTPase DRP-1.[23–25] In general, conditions that compromise mitochondrial membrane potential induce fragmentation and vesiculation of the mitochondrial network.[26,27] Indirect drug actions can also lead to mitochondrial network fragmentation, as evidenced by mitochondrial vesiculation caused by ouabain, which is an inhibitor of plasma membrane Na/K-ATPase.[23] In this case, mitochondrial effects of ouabain were reported to be cell-type dependent, occurring in CV-1, but not HeLa cells. We found that the strong LT–DMAPs induce mitochondrial network fragmentation in every type of cell we have so far examined, which includes over ten normal and malignant cell lines of mouse, human, and teleost origin (data not shown), suggesting that mitochondria are a direct target of these compounds.

Changes in mitochondrial TMRM fluorescence intensity after LT–DMAP exposure were quantitated using flow cytometry methods. Treatment of cells under conditions comparable to the fluorescence microscope studies (4 μg/ml LT–DMAP for 6 h) demonstrates that compounds **1–6** do not significantly reduce mitochondrial TMRM labeling intensity (Fig. 4). In fact, some of these compounds appear to slightly increase TMRM signal strength in WM793 cells, suggesting that mitochondrial membranes perhaps become slightly hyperpolarized in the presence of these compounds. Compounds **8** and **10** significantly reduce mitochondrial polarization in WM3211 cells, but not WM793 cells. Compounds **7** and **9** reduce TMRM fluorescence in both cell lines, with stronger effects again in the WM3211 cells. Compounds **11–15** significantly reduce TMRM fluorescence in both cell lines. In some experiments, the extent of mitochondrial depolarization was compared to that obtained with 20 μM of the ionophore carbonyl cyanide-*p*-trifluoromethoxyphenylhydrazone (FCCP). The values of the strong LT–DMAPs were consistently at or below the FCCP value (not shown). It should be noted that a reduction in fluorescence inten-

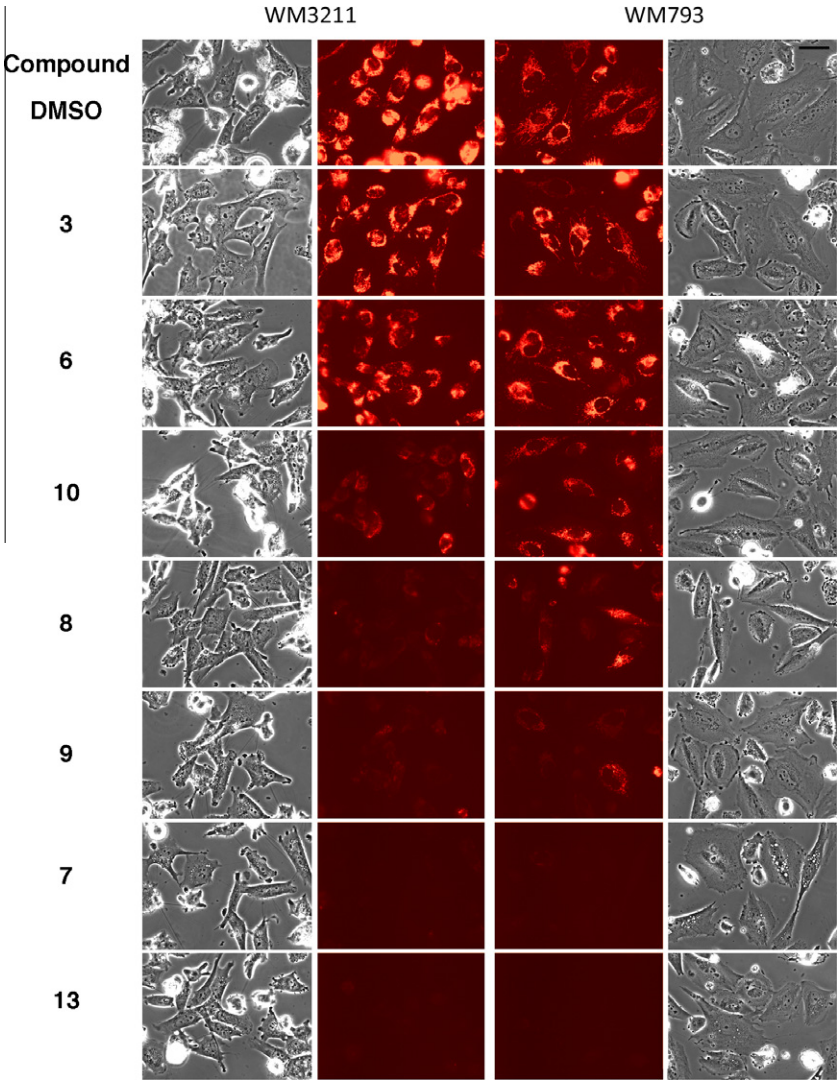

Figure 2. Morphology and mitochondrial polarization of WM3211 and WM793 cells treated with representative LT–DMAPS at 4 μg/ml for 5 h, and then labeled with TMRM. The same field of view for each sample is shown by both phase contrast and epifluorescence microscopy. Note that compound **3** (representative of the weak group) does not markedly influence cell or mitochondrial morphology or mitochondrial membrane polarization. The intermediate strength compounds **6**–**10** show a range of effects on mitochondria at this concentration and time point, with significant loss of mitochondrial membrane polarization with the strongest compounds of this group (**8**, **9** and **7**). The strong group all resulted in fragmentation and essentially complete depolarization of mitochondria, represented by **13**. All fluorescence images were photographed and rendered using identical camera settings and software methods to allow for direct comparison of fluorescence labeling strength. Bar (top right image) represents 20 μm.

sity measured by flow cytometry to about 20–30% of control cells corresponded to an essentially complete lack of mitochondrial fluorescence by epifluorescence microscopy. In general, there was excellent agreement between the mitochondrial fluorescence values measured by flow cytometry and the fluorescence intensity observed by microscopy (compare Figs. 2 and 4).

Based on the strength of mitochondrial effects (as well as effects on proliferation, see below), the 15 DMAP derivatives of triterpenoids can be grouped into three general categories: (i) **1–5** are very weak mitochondrial perturbants; (ii) **6–10** are intermediate in strength; and (iii) **11–15** are very strong, resulting in fragmentation and depolarization of mitochondria at concentrations under 4 μg/ml. Interestingly, both the weak and strong groups exhibit similar effects on both melanoma cell lines tested, whereas some members of the intermediate group (ii) exhibit some specificity, with the radial melanoma cell line WM3211 displaying greater sensitivity than the vertical WM793 cell line. In this group, the compounds **7, 8** and **10** showed the largest differences in effects between the two cell lines.

2.5. Effects of LT–DMAPs on cell proliferation

Dose–response sulforhodamine B (SRB) assays were used to test for effects of LT–DMAPs on cell proliferation. Similar to the effects on mitochondrial polarization, the effects of LT–DMAPs on cell proliferation could be grouped into strong, intermediate, and weak effects. Representative of the weak group, up to 4 μg/ml of compound **3** exhibited little effect on cell proliferation over three days of treatment (Fig. 5). Compound **6** was the weakest of the intermediate group, and inhibited proliferation to between 40% and 50% of controls at 4 μg/ml after three days; other members of this group strongly inhibited proliferation at concentrations over 2 μg/ml. Members of the strong group of compounds inhibited proliferation at concentrations over 0.5 μg/ml. Notably, members of the intermediate group once again showed distinct effects between the cell lines, with the radial-phase WM3211 cells being more sensitive to growth inhibition than the vertical-phase WM793 cells. In some experiments, a non-transformed cell line (BJ foreskin fibroblasts) was included to compare with the melanoma cell lines. Again,

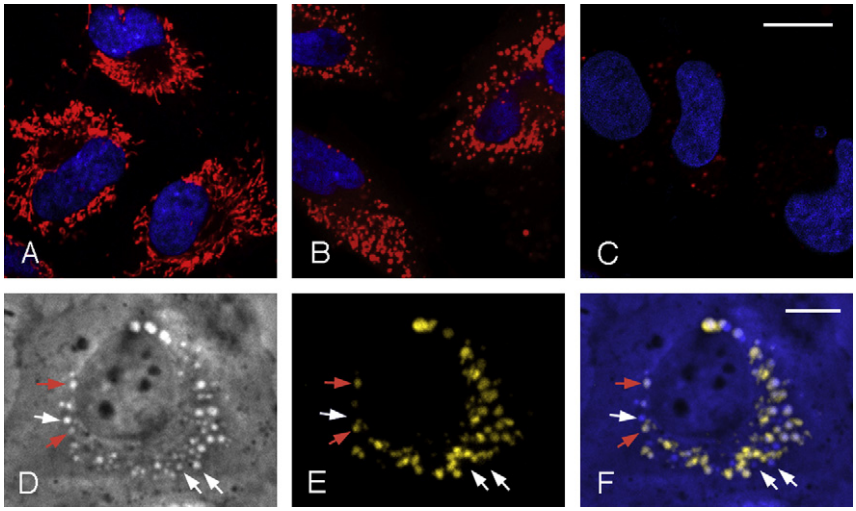

Figure 3. Effects of representative LT–DMAPs on WM793 mitochondrial structure and polarization. (A–C) Confocal microscopy of cells double-labeled with Hoechst 33342 to label nuclei (blue) and TMRM to label polarized mitochondria (red). (A) DMSO control; (B) cells treated with **10** at 4 μg/ml for 5 h; (C) cells treated with **15** at 4 μg/ml for 5 h. Note the distinct fragmentation of mitochondria with both compounds, and the almost complete loss of membrane polarization with **15**. (D–F) phase contrast and epifluorescence microscopy of the same cell, treated with **10** at 4 μg/ml for 5 h. In this higher magnification micrograph, the phase contrast image shown in D was colorized blue in F. The red TMRM signal was colorized yellow (E), and the two overlaid in F to better distinguish between TMRM-negative (blue in F) and TMRM-positive (yellow in F) vacuoles. This demonstrates that the vacuoles visible by phase contrast microscopy (arrows in D) are comprised of both labeled (red arrows) and unlabeled (white arrows) subpopulations. The labeled vacuoles presumably represent swollen mitochondria, based on the residual TMRM labeling. The unlabeled vacuoles could represent either more damaged and completely depolarized mitochondria, or, alternatively, non-mitochondrial structures such as swollen cisternae of the endoplasmic reticulum. A–C are the same magnification; bar in C represents 10 μm. D–F are the same magnification; bar in F represents 5 μm.

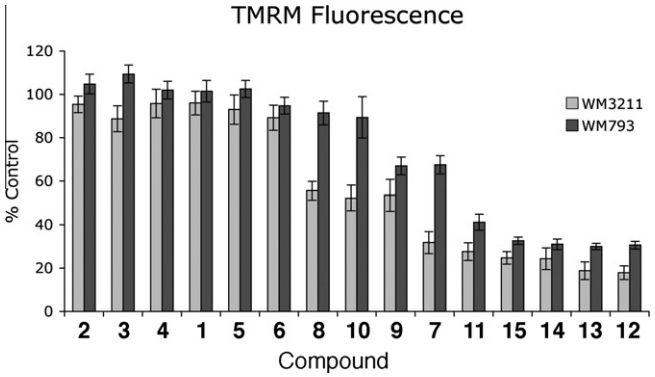

Figure 4. Quantitation of mitochondrial polarization (TMRM fluorescence) by flow cytometry. Cells were treated with compounds **1**–**15** at 4 μg/ml for 5 h, and subsequently labeled with TMRM and analyzed by flow cytometry. Fluorescence values are expressed as percent control (DMSO only vehicle control) for each cell line, which was set to 100%. Note that the progressive loss of mitochondrial polarization (reduction in TMRM fluorescence intensity) is more accentuated in the WM3211 cell line. The values between 20% and 40% for both cell lines exhibited by compounds **11**–**15** correspond to an essentially complete lack of visually-detectable labeling by epifluorescence microscopy (see Fig. 2). Values reflect the mean of three independent experiments; error bars indicate standard error of the mean.

differences in cell behavior were noted in the intermediate group. For example, BJ fibroblasts were more sensitive to **10** than WM793 cells, but less sensitive than WM3211 cells (Fig. 5). Similar to both melanoma cell lines, the weak group of LT–DMAPs exhibited little effect on BJ cell proliferation (not shown), and the strong group inhibited BJ growth to about the same extent as both melanoma lines (Fig. 5). The ED_{50} concentrations (the concentration of compound that inhibits cell proliferation to 50% of the vehicle-only control cells), calculated from the dose–response graphs, are listed in Table 1.

2.6. Correlation between mitochondrial depolarization and cell proliferation

The similarity of effects of the three groups (weak, intermediate, and strong) of LT–DMAPs on both mitochondrial polarization and cell proliferation suggests that the effect of these compounds is primarily mitochondrial, and that the inhibition of proliferation results from perturbation of mitochondrial structure and function. To examine this possibility more closely, TMRM fluorescence was plotted against the ED_{50} proliferation values (Fig. 6). For both cell lines, correlation of compounds with proliferation ED_{50}s under 4 μg/ml with mitochondrial TMRM fluorescence intensity displayed a Pearson coefficient of 0.854. This coefficient was 0.767 for the WM3211s, and 0.899 for the WM793s. From the plot, four points deviated somewhat from the trendline, and included compound **7** for WM793 cells, **8** for WM3211 cells, and **10** for both WM793 and WM3211 cells. Without these four data points, the Pearson coefficient rises to 0.966. Interestingly, these four points all belong to the intermediate group of LT–DMAPs. Overall, the strong correlation between mitochondrial TMRM fluorescence intensity and proliferative capacity suggest that the effects of these compounds on cell proliferation are primarily due to their disruptive effects on mitochondria. However, the fact that the compounds that best distinguish between radial and vertical cell lines also tend to lie furthest from the trendline raises the possibility that the ability of these compounds to differentially target the radial and vertical melanoma cell lines is due to additional, non-mitochondrial affects.

Examination of cultures by phase contrast microscopy during the drug treatment experiments revealed a notable level of cell death in cultures treated with higher concentrations of the strong group of compounds **11–15** after a few days of exposure (not shown). In these wells, the inhibition of proliferation clearly included cell death as a factor. However, little or no cell death was evident in cultures treated with lower concentrations of the strong group, or with the medium and weak groups over the time course studied (three days of treatment). Therefore, these compounds are also able to inhibit proliferation by slowing or arresting the cell cycle. Mitochondrial effects could explain both cell cycle inhibitions due to depletion of ATP levels, as well as induction of cell death by the intrinsic pathway of apoptosis. Triterpenoids reported to lead to a reduction in intracellular ATP levels include dehydroeburicoic acid, toosendanin, and avicin D.[16,28,29] Avicin D has

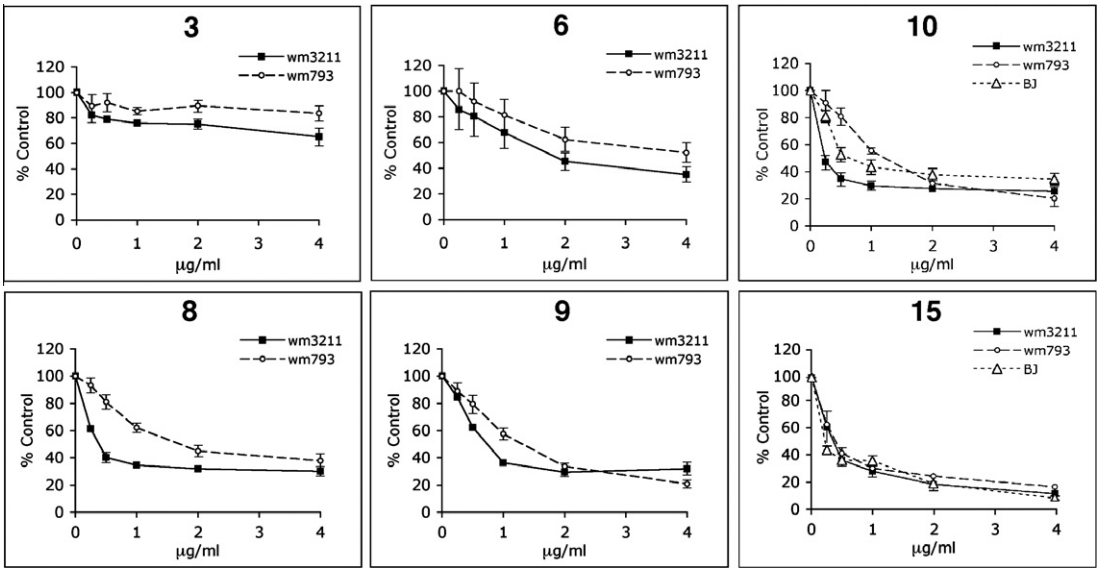

Figure 5. SRB dose–response curves for cell proliferation in the presence of LT–DMAPs. Values are shown as percent of controls (DMSO vehicle only; set to 100%) after three days of treatment. Representative compounds are shown, spanning effects from little inhibition of proliferation **3** to significant effects at less than 1 µg/ml (**10**, **8**, **9** and **15**). For **10** and **15**, effects on the normal (untransformed) BJ fibroblast cell line are also shown. In general, the largest differences of effects on proliferation based on cell type were exhibited by the intermediate strength compounds **6**–**10**.

Table 1
ED_{50} values for LT–DMAP compounds

Compound	WM3211 (µg/ml)	WM3211 (µM)	WM793 (µg/ml)	WM793 (µM)
1	>4	>6.1	>4	>6.1
2	>4	>4.4	>4	>4.4
3	>4	>4.7	>4	>4.7
4	>4	>3.5	>4	>3.5
5	>4	>3.8	>4	>3.8
6	1.8	2.6	4	5.7
7	0.5	0.8	1.7	2.6
8	0.4	0.6	1.7	2.5
9	0.7	0.7	1.3	1.3
10	0.2	0.3	1.2	1.9
11	0.5	0.6	0.7	0.8
12	0.3	0.3	0.5	0.5
13	0.4	0.5	0.4	0.5
14	0.4	0.4	0.4	0.4
15	0.4	0.5	0.4	0.5

Values represent the concentration (both in µg/ml and µM) required to inhibit cell proliferation to 50% of the control value over three days of culture after addition of compound. Values were derived from graphs representing the mean of three independent experiments.

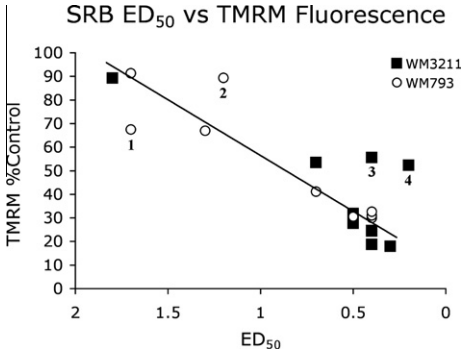

Figure 6. Graph plotting inhibition of proliferation (ED_{50}, *X*-axis) versus mitochondrial polarization (TMRM fluorescence, *Y*-axis). ED_{50} values were from Table 1, and mitochondrial fluorescence values were from Fig. 4. Pearson coefficients were calculated using Microsoft Excel. Compounds for the four points that lie somewhat off the trendline are: point 1 = **7**; point 2 = **10**; point 3 = **8**; point 4 = **10**. In general, there is very good agreement between loss of mitochondrial fluorescence and inhibition of cell proliferation.

been shown to activate the AMPK pathway,[16] which is involved in coordinating cellular energy charge with growth and proliferation.[30] Conversely, some triterpenoids have also been reported to enhance ATP levels and protect mitochondria from chemical insult.[31,32] It is likely that the effects of triterpenoids on cellular energy charge depend upon the specific features of the triterpenoid, the type of cell, and the metabolic state of the cell. In addition to affecting cell proliferation rates through effects on energy metabolism, some triterpenoids are associated with alterations in the expression patterns of cell cycle regulatory proteins such as cyclins, MYC, p21 and p27.[11,15,33–36] The extent to which these effects on cell cycle regulatory proteins are direct or indirect remain unclear at present.

Cell proliferation can also be reduced by upregulating cell death pathways, and mitochondria play central roles in the intrinsic pathway of apoptosis. The pentacyclic triterpenoid betulinic acid (BA) has been shown to exert direct effects on mitochondria, increasing mitochondrial membrane permeability and triggering the permeability pore transition.[37] BA causes mitochondrial depolarization and apoptotic cell death, which can be blocked by overexpression of Bcl-2 or bongkrekic acid, and thus is suggested to involve activation of the permabilization pore.[37,38] BA increases ROS production, which appears to be upstream of pore formation and initiation of apoptosis.[6,7,38,39] Interestingly, it has been suggested that some compounds may lead to mitochondrial permeabilization through unregulated mechanisms, including the formation of membrane aggregates that form hydrophilic channels,[40] and evidence for the ability of the synthetic triterpenoid CDDO to act in this way has been reported.[41] Preliminary experiments indicate that co-treatment with cyclosporin A does not reduce mitochondrial network fragmentation induced by the strong group of LT–DMAPs (data not shown), raising the possibility that these compounds are also able to act at least in part via non-regulated pore formation.

2.7. Structure–activity relationships in LT–DMAP mitochondrial disruption

Organic ions can penetrate biological membranes if the charge is delocalized or screened by hydrophobic moieties, and the polarized nature of mitochondria can accumulate high concentrations of charged molecules that are membrane permeable.[42] In particular, a variety of lipophilic cations have been shown to be concentrated effectively by mitochondria.[43,44] In this study, triterpenoids derivatized with one, two, or three DMAP groups were compared in their ability to disrupt mitochondria and suppress cell proliferation, and a few notable patterns emerged. The strongest compounds all possessed two DMAP groups, but those with three DMAP groups were generally not as effective. Mono-DMAP compounds exhibited a range of efficacies, and some of these displayed different potencies with respect to the radial and vertical melanoma cell lines. Preliminary screening of a number of DMAP compounds with a linear aliphatic chain substituted for the pentacyclic triterpenoid core indicates that these molecules are not very effective in either disrupting mitochondrial structure or inhibiting cell proliferation. This suggests that the triterpenoid portion is a critical element in the LT–DMAP anti-mitochondrial actions. It is currently unclear precisely how the triterpenoid skeleton is functioning, but it is likely that its lipophilicity contributes to the membrane permeability of these molecules. It is possible that the presence of two dimethylaminopiridinium groups anchors LT–DMAPs to mitochondrial membranes more effectively than a single group, whereas three such charged groups begins to inhibit the ability of these molecules to penetrate membranes, resulting in reduced potency. Along with the tri-DMAPs, di-DMAP molecules with C28-carboxylic acid derivatives are also less effective, again perhaps due to reduced membrane permeability. It is noteworthy that the potent di-DMAP compounds **11** and **12** had their dimethylaminopiridinioacetoxy groups at C28- and β-C3 positions, on the same (β) side of the triterpenoid molecule plane. Such a stereochemistry could facilitate membrane interactions of both active coordination sites, presumably leading to more effective membrane depolarization and subsequent mitochondrial fragmentation. To test for possible contributions of counter-ions to compound activity, compound pairs **2** and **3**, and **14** and **15** were synthesized so that they differed only in the counter ion (Br^- or Cl^-) present. Little or no difference in compound activity was noted within these pairs, suggesting that the effects on proliferation and mitochondrial structure and function are independent of the type of counter-ion.

High concentrations of cations in mitochondria have previously been shown to lead to an increase in the permeability of the inner mitochondrial membrane, non-specifically inhibit mitochondrial enzymes, reduce ATP levels, and facilitate cell death pathways.[43] The higher apparent polarization state of WM3211 mitochondria (based on TMRM labeling intensity) raises the possibility that they may accumulate mono- and di-DMAPs to a higher degree than WM793s, which could explain their greater sensitivity to some of these compounds.

3. Conclusion

Dimethylaminopyrimidine derivatives of lupane triterpenoids (LT–DMAPs) can be potent disruptors of mitochondrial structure and function. LT–DMAPs can also inhibit cell proliferation, and of the compounds tested in this study, their ability to inhibit proliferation is strongly correlated with their ability to disrupt mitochondria. The 15 compounds examined in this study fall into three general categories of weak, intermediate, and strong, based on their potency and ability to exert distinct effects on different cell lines. Structure–activity data indicates that the potency of these compounds is not simply related to the number of DMAP groups present. The weak group included BA derivatives possessing one, two and three DMAP groups; however, the strongest compounds all contained two DMAP groups. Interestingly, the compounds that best distinguished between the radial and vertical phase melanoma cell lines were all mono-DMAPs. Although some differences in responses were observed between the cell lines (especially among the mono-DMAPs), a more meaningful demonstration of bioselectivity will require the comparison of larger numbers of cell lines and tumor types in both in vitro and in vivo settings.

4. Experiments

Melting points were determined on an Original Mel-Temp Laboratory devices INC apparatus (USA). The ^{1}H NMR spectra were recorded with a Varian 500 MHz, the deuterated solvents indicated were used. Chemical shifts are reported in parts per million (ppm) relative to TMS. TLC was run on the silica gel coated aluminum sheets (Silica Gel 60 $GF_{254,}$ E. Merk, Germany) and visualized in UV light (254 nm). All chemicals and solvents were purchased from Aldrich Chemical or Acros Organics and dried by standard procedure.

4.1. Synthesis

4.1.1. O-acylation of betulin (16) and betulinic acid (18)

The following chloro- and bromocarboxylic acids chlorides or bromides have been used as a reagents for O-acylation: Reagent (20 mmol) was added to a solution of betulin or betulinic acid (5–10 mmol) in 30–50 ml of *N*,*N*-dimethylacetamide (DMA). Reaction mixture was stirred for 24 h at rt. Benzene (70–100 ml) was added to reaction mixture, washed with 10% $KHCO_3$ (2 × 15 ml) and water (3 × 10 ml), dried over Na_2SO_4 and evaporated under reduced pressure. The residue was purified on silica with hexane/Et_2O (4:1). Yielded white crystals (95%) were subjected to the reaction of quaternization with DMAP.

4.1.2. Bromination of O-acetylated LT

NBS (20 mmol) and ABIN (1 mmol) were added to the solution of O-acetylated LT (3 mmol) in 80 ml of dry CCl_4. Reaction mixture was refluxed for 20 min, stirred at rt for 8 h and filtered. Solvent was removed in vacuum. Residue was crystallized from 2-propanol, yielded 83–86% off-white crystals.

4.1.3. Quaternization with DMAP

To a solution of O-acylated and/or brominated LT (3 mmol) in DMA (15 ml) was added in one portion DMAP (6–20 mmol). Reaction mixture was stirred for 10 h at 60 °C. After cooling to rt diethyl ether (20–30 ml) was added, precipitate was separated, washed with diethyl ether 2 × 15 ml and dried in vacuum.

4.1.4. Characteristics of synthesized LT QUATS (1–15)

4.1.4.1. 3β-hydroxy-30-(4-dimethylaminopyridinio)lup-20-en-28-oic acid bromide (1). ^{1}H NMR (500 MHz, CD_3OD): δ = 8.11 (d, 2H), 7.02 (d, 2H), 4.78 (s, 1H), 4.71 (s, 1H), 3.27 (s, 6H), 3.11 (m, 1H), 2.37 (t, 1H), 2.23 (d, 1H), 2.0–0.68 (m, 42H). Mp 192–193 °C. HRMS (ESI^+) MH^+: 657.3628 (calcd mass for $C_{55}H_{82}Br_3N_6O_4^+$: 657.3625).

4.1.4.2. 3β-[2-(4-Dimethylaminopyridinio)acetoxy]-30-(4-dimethylaminopyridinio)lup-20-en-28-oic acid dibromide (2). ^{1}H NMR (500 MHz, CD_3OD): δ = 8.1 (d, 4H), 7.03 (d, 4H), 5.11 (m, 2H), 4.79 (s, 1H), 4.69 (s, 1H), 4.57 (m, 1H), 4.5 (m, 2H), 3.28 (s, 12H), 2.9 (m, 1H), 2.4 (m, 1H), 2.23 (d, 1H), 2.04–0.53 (m, 38H). Mp 105–106 °C. HRMS (ESI^+) MH^+: 899.3683 (calcd mass for $C_{46}H_{69}Br_2N_4O_4^+$: 899.3680).

4.1.4.3. 3β-[2-(4-Dimethylaminopyridinio)acetoxy]-30-(4-dimethylaminopyridinio)lup-20-en-28-oic acid bromide chloride (3). ^{1}H NMR (500 MHz, CD_3OD): δ = 8.2 (d, 4H), 7.1 (d, 4H), 5.11 (m, 2H), 4.79 (s, 1H), 4.69 (s, 1H), 4.57 (m, 1H), 4.51 (m, 2H), 3.28 (s, 12H), 2.92 (m, 1H), 2.42 (m, 1H), 2.25 (d, 1H), 2.07–0.57 (m, 38H). Mp 93–94 °C. HRMS (ESI$^+$) MH$^+$: 855.4188 (calcd mass for $C_{46}H_{69}BrClN_4O_4^+$: 855.4185).

4.1.4.4. 3β,28-Di[2-(4-dimethylaminopyridinio)acetoxy]-30-(4-dimethylaminopyridinio)lup-20-en tribromide (4). ^{1}H NMR (500 MHz, CD_3OD): δ = 8.16 (d, 6H), 7.06 (d, 6H), 5.18 (m, 4H), 4.82 (s, 1H), 4.65 (s, 1H), 4.55 (m, 1H), 4.5 (d, 1H), 4.0 (d, 1H), 3.29 (s, 12H), 3.28 (s, 6H), 2.4 (m, 1H), 2–0.75 (m, 41H). Mp 123–124 °C. HRMS (ESI$^+$) MH$^+$: 1127.3946 (calcd mass for $C_{55}H_{82}Br_3N_6O_4^+$: 1127.3942).

4.1.4.5. 3β,28-Di[2-(4-dimethylaminopyridinio)acetoxy]-30-(4-dimethylaminopyridinio)lup-20-en 29-bromide dichloride (5). ^{1}H NMR (500 MHz, CD_3OD): δ = 8.14 (d, 6H), 7.04 (d, 6H), 5.14 (m, 4H), 4.81 (s, 1H), 4.6 (s, 1H), 4.59 (m, 1H), 4.5 (d, 1H), 3.96 (d, 1H), 3.28 (s, 12H), 3.27 (s, 6H), 2.4 (m, 1H), 2–0.75 (m, 41H). Mp 120–121 °C. HRMS (ESI$^+$) MH$^+$: 1039.4955 (calcd mass for $C_{55}H_{82}BrCl_2N_6O_4^+$: 1039,4952).

4.1.4.6. 3β-[2-(4-Dimethylaminopyridinio)acetoxy]lup-20-en-28-oic acid bromide (6). ^{1}H NMR (500 MHz, CD_3OD): δ = 8.12 (d, 2H), 7.03 (d, 2H), 5.12 (m, 2H), 4.7 (s, 1H), 4.6 (s, 1H), 4.55 (m, 1H), 3.28 (s, 6H), 3.04 (m, 1H), 2.35 (t, 1H), 2.23 (d, 1H), 2.07–0.75 (m, 41H). Mp 292–293 °C. HRMS (ESI$^+$) MH$^+$: 699.3729 (calcd mass for $C_{39}H_{60}Br_3N_2O_4^+$: 699.3731).

4.1.4.7. 3β-Hydroxy-28-[2-(4-dimethylaminopyridinio)propanyloxy]lup-20-en-28-ol chloride (7). ^{1}H NMR (500 MHz, CD_3OD): δ = 8.24 (d, 2H), 7.04 (d, 2H), 5.35 (dd, 1H), 4.71 (s, 1H), 4.6 (s, 1H), 4.5 (dd, 1H), 3.99 (dd, 1H), 3.28 (s, 6H), 3.11 (dd, 1H), 2.44 (m, 1H), 2–0.69 (m, 46H). Mp 222–223 °C. HRMS (ESI$^+$) MH$^+$: 655.4604 (calcd mass for $C_{40}H_{64}ClN_2O_3^+$: 655.4600).

4.1.4.8. 3β-[2-(4-Dimethylaminopyridinio)acetoxy]lup-20-en-28-ol bromide (8). ^{1}H NMR (500 MHz, $CDCl_3$): δ = 8.12 (d, 2H), 7.03 (d, 2H), 5.1 (m, 1H), 4.68 (s, 1H), 4.61 (d, 1H), 4.56 (s, 1H), 3.73 (d, 1H), 3.28 (s, 6H), 2.44 (m, 1H), 2.07–0.75 (m, 45H). Mp 292–293 °C. HRMS (ESI$^+$) MH$^+$: 685.3935 (calcd mass for $C_{39}H_{62}BrN_2O_3^+$: 685.3938).

4.1.4.9. 3β,28-Di[4-(4-dimethylaminopyridinio)butyryloxy]lup-20-en dibromide (9). ^{1}H NMR (500 MHz, CD_3OD): δ = 8.17 (d, 4H), 7.01 (d, 4H), 4.69 (d, 1H), 4.57 (d, 1H), 4.4 (d, 1H), 4.23 (m, 4H), 3.8 (d, 1H), 3.28 (s, 12H), 2.42 (m, 5H), 2.15 (m, 4H), 2–0.75 (m, 43H). Mp 149–150 °C. HRMS (ESI$^+$) MH$^+$: 983.4621 (calcd mass for $C_{52}H_{81}Br_2N_4O_4^+$: 983.4619).

4.1.4.10. 3β-[2-(4-Dimethylaminopyridinio)acetoxy]lup-20-en-28-ol chloride (10). ^{1}H NMR (500 MHz, $CDCl_3$): δ = 8.12 (d, 2H), 7.03 (d, 2H), 5.1 (m, 2H), 4.68 (s, 1H), 4.57 (m, 1H), 4.55 (s, 1H), 3.72 (d, 1H), 3.28 (s, 6H), 2.44 (m, 1H), 2.07–0.82 (m, 44H). Mp 289–290 °C. HRMS (ESI$^+$) MH$^+$: 641.4445 (calcd mass for $C_{39}H_{62}Br_3N_2O_3^+$: 641.4443).

4.1.4.11. 3β,28-Di[3-(4-dimethylaminopyridinio)propionyloxy]-lup-20-en dichloride (11). ^{1}H NMR (500 MHz, CD_3OD): δ = 8.21 (d, 4H), 6.99 (d, 4H), 4.69 (d, 1H), 4.57 (d, 1H), 4.46 (m, 4H), 4.4 (d, 1H), 3.8 (d, 1H), 3.28 (s, 12H), 2.99 (m, 4H), 2.42 (m, 1H), 2–0.75 (m, 43H). Mp 140–141 °C. HRMS (ESI$^+$) MH$^+$: 867.5319 (calcd mass for $C_{50}H_{77}Cl_2N_4O_4^+$: 867.5316).

4.1.4.12. 3β,28-Di[2-(4-dimethylaminopyridinio)butyryloxy]lup-20-en dibromide (12). ^{1}H NMR (500 MHz, $CDCl_3$): δ = 8.23 (d, 4H), 7.06 (d, 4H), 5.17 (dt, 1H), 5.01 (dd, 1H), 4.69 (d, 1H), 4.58 (d, 1H), 4.49 (d, 1H), 4.0 (d, 1H), 3.29 (s, 12H), 2.39 (m, 3H), 2.19 (m, 2H), 2–0.75 (m, 49H). Mp 157–158 °C. HRMS (ESI$^+$) MH$^+$: 983.4616 (calcd mass for $C_{55}H_{81}Br_2N_4O_4^+$: 983.4619).

4.1.4.13. 3β,28-Di[2-(4-dimethylaminopyridinio)propanyloxy]lup-20-en dichloride (13). ^{1}H NMR (500 MHz, CD_3OD): δ = 8.22 (d, 4H), 7.03 (d, 4H), 5.33 (dd, 2H), 4.71 (s, 1H), 4.6 (s, 1H), 4.55 (dd, 1H), 4.45 (d, 1H), 4.0 (d, 1H), 3.28 (s, 12H), 2.46 (m, 1H), 2–0.75 (m, 48H). HRMS (ESI$^+$) MH$^+$: 867.5318 (calcd mass for $C_{50}H_{77}Cl_2N_4O_4^+$: 867.5316).

4.1.4.14. 3β,28-Di[2-(4-dimethylaminopyridinio)acetoxy]lup-20-en dibromide (14). ^{1}H NMR (500 MHz, CD_3OD): δ = 8.11 (d, 4H), 7.02 (d, 4H), 5.11 (m, 4H), 4.71 (s, 1H), 4.6 (s, 1H), 4.56 (m, 1H), 4.51 (d, 1H), 4.01 (d, 1H), 3.28 (s, 12H), 2.47 (m, 1H), 2.07–0.82 (m, 42H). Mp 227–228 °C. HRMS (ESI$^+$) MH$^+$: 927.3991 (calcd mass for $C_{48}H_{73}Br_2N_4O_4^+$: 927.3993).

4.1.4.15. 3β,28-Di[2-(4-dimethylaminopyridinio)acetoxy]lup-20-en dichloride (15). ^{1}H NMR (300 MHz, CD_3OD): δ = 8.14 (d, 4H), 7.04 (d, 4H), 5.14 (m, 4H), 4.72 (s, 1H), 4.6 (s, 1H), 4.57 (m, 1H), 4.52 (d, 1H), 4.02 (d, 1H), 3.28 (s, 12H), 2.47 (m, 1H), 2.07–0.82 (m, 42H). Mp 226–227 °C. HRMS (ESI$^+$) MH$^+$: 839.5005 (calcd mass for $C_{48}H_{73}Cl_2N_4O_4^+$: 839.5003).

4.2. Mitochondrial labeling

For microscopy, cells were plated on glass-bottom cell culture dishes (Mat-Tek Inc.) and allowed to grow until approximately 30% confluent. Compounds were all added at a final concentration of 4 μg/ml, and cells incubated for 5 h in a cell culture incubator. Vehicle-only controls received an equivalent amount of dimethylsulfoxide (DMSO) only, which corresponded to a concentration of 0.2%. Tetramethylrhodamine methylester (TMRM; Sigma Chem. Co.) was added to a final concentration of 100 nM, and cells incubated further for 60 min. Culture medium/TMRM was then aspirated and replaced with PBS containing 5% Fetal Clone III, and dishes immediately examined and photographed on an inverted Nikon TE-2000 epifluorescence microscope equipped with an Coolsnap ES camera (Photometrics).

For flow cytometry, cells were suspended in 0.5 ml aliquots of culture medium at a density of 30,000 cells/ml. Compound addition and TMRM labeling was carried out as described for microscopy, above, with the exception that after the TMRM incubation period, cells were immediately analyzed by flow cytometry without medium replacement. TMRM fluorescence intensity was measured using the FL2 channel of a Becton-Dickenson FACScalibur, and plotted against size (forward scatter). Mean fluorescence intensity was obtained from identically-sized gated regions.

Acknowledgements

This study was supported by a grant from the Whiteside Institute for Clinical Research to J.H. and P.A.K., a research grant from the University of Minnesota—Duluth to P.A.K., and a research grant from the Portuguese Foundation of Science and Technology to P.J.O. (PTDC/QUI/101409/2008).

References and notes

1. Krasutsky, P. *Nat. Prod. Rep.* **2006**, *23*, 919.
2. Petronelli, A.; Pannitteri, G.; Testa, U. *Anticancer Drugs* **2009**, *20*, 880.
3. Pisha, E.; Chai, H.; Lee, I. S.; Chagwedera, T. E.; Farnsworth, N. R.; Cordell, G. A.; Beecher, C. W.; Fong, H. H.; Kinghorn, A. D.; Brown, D. M., et al *Nat. Med.* **1995**, *1*, 1046.

4. Zuco, V.; Supino, R.; Righetti, S. C.; Cleris, L.; Marchesi, E.; Gambacorti-Passerini, C.; Formelli, F. *Cancer Lett.* **2002**, *175*, 17.
5. Fulda, S.; Jeremias, I.; Steiner, H. H.; Pietsch, T.; Debatin, K. M. *Int. J. Cancer* **1999**, *82*, 435.
6. Wick, W.; Grimmel, C.; Wagenknecht, B.; Dichgans, J.; Weller, M. *J. Pharmacol. Exp. Ther.* **1999**, *289*, 1306.
7. Fulda, S.; Friesen, C.; Los, M.; Scaffidi, C.; Mier, W.; Benedict, M.; Nunez, G.; Krammer, P. H.; Peter, M. E.; Debatin, K. M. *Cancer Res.* **1997**, *57*, 4956.
8. Fulda, S.; Susin, S. A.; Kroemer, G.; Debatin, K. M. *Cancer Res.* **1998**, *58*, 4453.
9. Fulda, S.; Debatin, K. M. *Med. Pediatr. Oncol.* **2000**, *35*, 616.
10. Laszczyk, M. N. *Planta Med.* **2009**, *75*, 1549.
11. Liby, K. T.; Yore, M. M.; Sporn, M. B. *Nat. Rev. Cancer* **2007**, *7*, 357.
12. Deeb, D.; Gao, X.; Jiang, H.; Dulchavsky, S. A.; Gautam, S. C. *Prostate* **2009**, *69*, 851.
13. Jutooru, I.; Chadalapaka, G.; Chintharlapalli, S.; Papineni, S.; Safe, S. *Mol. Carcinog.* **2009**, *48*, 692.
14. Pathak, A. K.; Bhutani, M.; Nair, A. S.; Ahn, K. S.; Chakraborty, A.; Kadara, H.; Guha, S.; Sethi, G.; Aggarwal, B. B. *Mol. Cancer Res.* **2007**, *5*, 943.
15. Thoennissen, N. H.; Iwanski, G. B.; Doan, N. B.; Okamoto, R.; Lin, P.; Abbassi, S.; Song, J. H.; Yin, D.; Toh, M.; Xie, W. D.; Said, J. W.; Koeffler, H. P. *Cancer Res.* **2009**, *69*, 5876.
16. Xu, Z. X.; Liang, J.; Haridas, V.; Gaikwad, A.; Connolly, F. P.; Mills, G. B.; Gutterman, J. U. *Cell Death Differ.* **2007**, *14*, 1948.
17. PCT/US2007/066896.
18. PCT/US2006/011794.
19. U.S. Patent 7410,958, 2008.
20. IV, K. *Nat. Prod. Commun.* **2007**, *2*.
21. Skehan, P.; Storeng, R.; Scudiero, D.; Monks, A.; McMahon, J.; Vistica, D.; Warren, J. T.; Bokesch, H.; Kenney, S.; Boyd, M. R. *J. Natl. Cancer Inst.* **1990**, *82*, 1107.
22. Skulachev, V. P.; Bakeeva, L. E.; Chernyak, B. V.; Domnina, L. V.; Minin, A. A.; Pletjushkina, O. Y.; Saprunova, V. B.; Skulachev, I. V.; Tsyplenkova, V. G.; Vasiliev, J. M.; Yaguzhinsky, L. S.; Zorov, D. B. *Mol. Cell Biochem.* **2004**, *256 and 257*, 341.
23. Pletjushkina, O. Y.; Lyamzaev, K. G.; Popova, E. N.; Nepryakhina, O. K.; Ivanova, O. Y.; Domnina, L. V.; Chernyak, B. V.; Skulachev, V. P. *Biochim. Biophys. Acta* **2006**, *1757*, 518.
24. Legros, F.; Lombes, A.; Frachon, P.; Rojo, M. *Mol. Biol. Cell* **2002**, *13*, 4343.
25. De Vos, K. J.; Allan, V. J.; Grierson, A. J.; Sheetz, M. P. *Curr. Biol.* **2005**, *15*, 678.
26. Cereghetti, G. M.; Stangherlin, A.; Martins de Brito, O.; Chang, C. R.; Blackstone, C.; Bernardi, P.; Scorrano, L. *Proc. Natl. Acad. Sci. U.S.A.* **2008**, *105*, 15803.
27. Wasilewski, M.; Scorrano, L. *Trends Endocrinol. Metab.* **2009**, *20*, 287.
28. Deng, J. Y.; Chen, S. J.; Jow, G. M.; Hsueh, C. W.; Jeng, C. J. *Chem. Res. Toxicol.* **2009**, *22*, 1817.
29. Zhang, Y.; Qi, X.; Gong, L.; Li, Y.; Liu, L.; Xue, X.; Xiao, Y.; Wu, X.; Ren, J. *Toxicology* **2008**, *249*, 62.
30. Hardie, D. G. *Nat. Rev. Mol. Cell Biol.* **2007**, *8*, 774.
31. Tian, J.; Zhang, S.; Li, G.; Liu, Z.; Xu, B. *Phytother. Res.* **2009**, *23*, 486.
32. Anbarasi, K.; Vani, G.; Devi, C. S. *J. Environ. Pathol. Toxicol. Oncol.* **2005**, *24*, 225.
33. Lapillonne, H.; Konopleva, M.; Tsao, T.; Gold, D.; McQueen, T.; Sutherland, R. L.; Madden, T.; Andreeff, M. *Cancer Res.* **2003**, *63*, 5926.
34. Lavhale, M. S.; Kumar, S.; Mishra, S. H.; Sitasawad, S. L. *PLoS One* **2009**, *4*, e5365.
35. Papineni, S.; Chintharlapalli, S.; Safe, S. *Mol. Pharmacol.* **2008**, *73*, 553.
36. Roy, M. K.; Kobori, M.; Takenaka, M.; Nakahara, K.; Shinmoto, H.; Tsushida, T. *Planta Med.* **2006**, *72*, 917.
37. Fulda, S.; Scaffidi, C.; Susin, S. A.; Krammer, P. H.; Kroemer, G.; Peter, M. E.; Debatin, K. M. *J. Biol. Chem.* **1998**, *273*, 33942.
38. Fulda, S.; Kroemer, G. *Drug Discovery Today* **2009**, *14*, 885.
39. Tan, Y.; Yu, R.; Pezzuto, J. M. *Clin. Cancer Res.* **2003**, *9*, 2866.
40. He, L.; Lemasters, J. J. *FEBS Lett.* **2002**, *512*, 1.
41. Brookes, P. S.; Morse, K.; Ray, D.; Tompkins, A.; Young, S. M.; Hilchey, S.; Salim, S.; Konopleva, M.; Andreeff, M.; Phipps, R.; Bernstein, S. H. *Cancer Res.* **2007**, *67*, 1793.
42. Skulachev, V. P. *Membrane Bioenergetics*; Springer: Berlin, 1988.
43. Murphy, M. P. *Trends Biotechnol.* **1997**, *15*, 326.
44. Modica-Napolitano, J. S.; Aprille, J. R. *Adv Drug Delivery Rev.* **2001**, *49*, 63.